Wasit Journal of Engineering Sciences

Journal homepage: https://ejuow.uowasit.edu.iq

# CFD simulation of helical coil heat exchanger with Different coil pitch to heating heavy fuel oil

Safaa A. Saleh[1], Zena K. Kadhim[1], and Kamil Abdulhusein Khalaf[1]

**Affiliations**
[1]Mechanical Engineering Department
College of Engineering, Wasit University
Kut, Iraq

**Correspondence**
Safaa A. Saleh
safaasalah302@uowasit.edu.iq

**Received**
7-August-2023
**Revised**
19-September-2023
**Accepted**
3-October-2023
Doi:
10.31185/ejuow.Vol11.Iss3.472

## Abstract

In this work Numerical investigations have been done for shell and helical tube heat exchanger using ANSYS FLUENT package 19. 2. It had been chosen as a heat recovery device in order to recover heat from exhaust gases of bricks factory furnaces and use it to preheat the heavy fuel oil and reduce fuel consumption. Air had been chosen as a hot gas instead of furnace exhaust gases because of the similar thermal properties. Numerical study involved design of helical tube with different curvature ratio (di/Dc) 0.166, 0.153, and 0.142 and different coil pitch (30, 50, 75, and 100) mm has been chosen. In shell side cold fluid (oil) "flow rate" is varying from (0.06 - 0.1) kg/s and velocity of hot fluid (air) changes from (20 - 48) m/s in helical tube with inlet temperature (200, 225, 250) °C. It has been found out that increasing "oil mass flow rate" from kg/s cause decreasing oil outlet temperature and curvature ratio 0.142 gives higher heat transfer rate while higher Dean number and Nusselt number in coil with curvature ratio 0.166. Also, results show increases of coil pitch led to increasing in overall heat transfer coefficient and Nusselt number of the shell side. while, heat transfer, oil outlet temperature effectiveness and pressure drop, decreases along helical tube. Finally, by investigating the temperature contour, it was determined that a secondary flow through the helical tube affected by centrifugal force, was existed, enhancing the fluid flow turbulency and heat transfer rate.

**Keywords:** shell and helical tube; pitch coil; coil diameter; Dean Number; curvature ratio; oil outlet temperature

**الخلاصة:**

في العمل الحالي ، تم إجراء محاكاة عددية للمبادل الحراري ذو الملف الحلزوني باستخدام برنامج ANSYS FLUENT 19.2 حيث يتم اختيار هذا المبادل كجهاز لاستعادة الحرارة الضائعة من اجل تسخين الزيت الثقيل وتقليل استهلاك الوقود في معامل الطابوق حيث تم اختيار الهواء بدل من غازات العوادم لانه يحمل نفس الخواص االحرارية. تضمنت الدراسة العددية تصميم مبادل حراري مكون من الاسطوانة ( القشرة ) ذو ملف حلزوني مع نسبة انحناء مختلفة ودرجة حلزنة محتلفة . تمت دراسة ثلاثة مبادلات حرارية ذات أنبوب حلزوني بنسب انحناء مختلفة 0.166 و 0.153 و 0.142 لاختيار الأفضل. تم اختيار أربعة ملفات حلزونية ذات درجة حلزنة مختلفة (30 ، 50 ، 75 ، 100) ملم . في الغلاف الجانبي للسائل البارد (الزيت) "معدل التدفق" يختلف من (0.06 - 0.1) كغم / ثانية ، وتتراوح سرعة (الهواء) الساخن من (20 إلى 48) م / ث في الأنبوب الحلزوني مع درجة حرارة الهواء (200 ، 225 ، 250) درجة مئوية. لقد وجد أن زيادة "معدل تدفق كتلة الزيت" من (0.06-0.1) كجم / ثانية يؤدي إلى خفض "درجة حرارة الزيت" حوالي 3٪ ونسبة الانحناء 0.142 تعطي معدل نقل حرارة أعلى ودرجة حرارة الزيت اكبر بينما يزداد رقم دين ورقم نسلت في الملف مع نسبة انحناء 0.166. أظهرت النتائج أيضًا أن زيادة درجة حلزنة الملف أدت إلى زيادة معامل انتقال الحرارة الكلي وعدد نسلت من جانب الغلاف بينما كمية الحرارة ، درجة حرارة الزيت ، فعالية المبادل الحراري وانخفاض الضغط ، يتناقص على طول الملف مع زيادة خطوة الملف .

## Nomenclature

| Symbol | Title | Units |
|---|---|---|
| $C$ | Heat capacity | *W/°C* |
| $C_{pc}$ | Specific heat of cold fluid | *J/kg. °C* |
| $C_{ph}$ | Specific heat of hot fluid | *J/kg. °C* |
| $D_c$ | Coil diameter | *m* |
| $d_i$ | Internal diameter of helical tube | *m* |
| $d_h$ | Hydraulic diameter | *m* |
| $De$ | Dean number | - |
| $f$ | Friction factor | - |
| $h_i$ | Inner side heat transfer coefficient | $W/m^2$. *°C* |
| $h_o$ | outer side heat transfer coefficient | $W/m^2$. *°C* |
| $K$ | Thermal conductivity | *W/m. °C* |
| $L$ | Tube length | *m* |
| $L_c$ | Helical tube length | *m* |
| $\dot{m}_c$ | Mass flow rate of cold fluid | *kg/sec* |
| $\dot{m}_h$ | Mass flow rate of hot fluid | *kg/sec* |
| $Nu$ | Nusselt number | - |
| $Pr$ | Prandtl number | - |
| $Q$ | Heat transfer rate | *W* |
| $Re$ | Reynolds number | - |
| $T$ | Temperature | *°C* |
| $\boldsymbol{T_{ci}}$ | Inlet temperature of cold fluid | *°C* |
| $\boldsymbol{T_{co}}$ | Outlet temperature of cold fluid | *°C* |
| $\boldsymbol{T_{hi}}$ | Inlet temperature of hot fluid | *°C* |
| $\boldsymbol{T_{ho}}$ | Outlet temperature of hot fluid | *°C* |
| p | pitch | *mm* |
| $U$ | Overall heat transfer coefficient | $W/m^2$. *°C* |
| $u_{ave}$ | Air velocity | *m/s* |

## Greek Symbols

| Symbol | Title | Units |
|---|---|---|
| $\Delta P$ | Pressure drops | *Pa* |
| $\Delta T$ | Temperature difference | *°C* |
| $\Delta T_m$ | mean temperature difference | *°C* |
| $\varepsilon$ | Heat exchanger effectiveness | - |
| $\mu$ | viscosity | *kg/m.sec* |
| $\mu_t$ | The turbulent eddy viscosity | *kg/m.sec* |
| $\rho$ | Fluid density | $kg/m^3$ |
| $\gamma$ | Pitch ratio | - |
| $\delta$ | Curvature ratio | - |

# 1. INTRODUCTION

The energy contained in one fluid must be transferred from one fluid to another using process equipment. A heat exchanger is a mechanical device that converts thermal energy from a hotter fluid to a colder fluid. In other ways, heat exchangers ensure that two fluids of varying temperatures effectively exchange heat while preventing the fluids from mixing due to a dividing wall. Heat exchangers are in common use in many engineering applications, such as air conditioning and refrigeration systems, space heating, Petro-chemical plants, waste heat recovery, natural gas processing, boilers, condensers, chemical processes, sewage treatment, power generation and automotive applications. Shell and helical tube heat exchangers are Common apparatus used in a variety of industrial settings, including those concerning nuclear power, chemical and food industries, solar energy applications. "Figure (1)" shown shell and helical tube heat exchanger which is the essential piece of engineering machinery for transferring heat from one fluid to another. These type of heat exchangers are becoming increasingly important nowadays. "Heat transfer rate" of "shell and helical tube heat exchangers" is significantly great because the secondary flow pattern innovative in helical coil due to "centrifugal force" caused by curvature of tube [1] Additionally, they have higher heat transfer coefficients and provide a larger heat transfer surface in a condensed space [2]. In industries, designing and thermal evaluating heat exchangers is often done to maximize heat transfer while minimizing cost, material, and energy use. Making a heat exchanger small and maximizing heat transmission with the least amount of space is the major difficulty in heat exchanger design. By creating secondary flow in the coil, the coiled tube passive enhancement approach has a great potential to improve heat transfer. Studying flow and heat transfer in helical coil tubes is essential due to improved heat transmission. The first challenge has been made by Dean to define mathematically the flow in a helical tube.

In this paper, will be used shell and helical tube for the purpose of heating heavy oil by hot air. The air flow is in the helical tube while, the heavy oil is in the shell. The effect of various geometrical parameters, such as curvature ratio, helical tube pitch, on heating of heavy oil are discussed. The results are given as temperature contours, average Nusselt number versus Dean number.

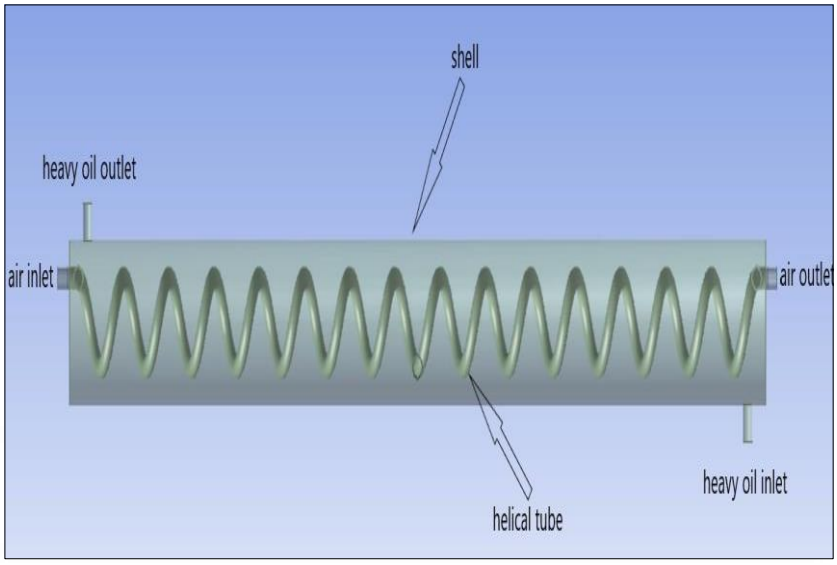


Fig.1 Shell and helical tube heat exchange

# 2. LITERATURE REVIEW

Theoretical and practical investigations on the waste heat recovery of combustion stack gas at about 200°C in vertical helical coils were given by **Kong et .al** [3]. This study used curvature ratios of 0.04 to 0.06 and pitch to coil diameter ratios of 0.1 to 0.25. The outcome shown that increasing curvature (d/D) or decreasing coil diameter enhanced the water side heat transfer coefficient and Nusselt number.

**Sheeba et.al** [4] calculated experimentally and numerically the effect of increasing Dean number in "helical tube heat exchanger" . According to research, heat transfer rates rise by 75% as Dean numbers increase from 325 to 600, and total heat transfer coefficient rises with pitch until it reaches a maximum at pitch 75 mm before falling.

The pressure drop of air flowing through helical tubes with different shapes and various coil sizes was experiment ally investigated by **Rezaei et.al** [5] .According to the study, the triangle, square, pentagon, and circle, respectively, display the biggest pressure drops while the flow rate and coil diameter remain constant.

In order to anticipate fluid flow and heat transfer characteristics using a combination of forced convection and "thermal radiation" in coil tubes, **Kushwaha et.al** [6] provided numerical analysis. The results showed an increase in curvature ratio led to increase friction factor and Nusselt number with an increase in Reynolds number due to effect of "thermal radiation" and "secondary flow"

**KUMAR** et.al,[7] studied experimentally effect "volume flow rate" on "overall heat transfer coefficient". The study showed effectiveness and temperature difference decreased with increased "volume flow rate" in coil side.

**Abu-Hamdeh** et.al, [8] used ANSYS FLUENT software to conduct analysis of performance of a "helical double-tube heat exchanger". Pitch (P) was selected between (0.5 – 30) mm and 30 mm length. The study's major findings are that shear stress lowers with increasing pitch and that overall heat transfer coefficient improved by 45%.

**Najm** et.al, [9] presented numerically helical "heat exchangers" with modified pitch coil to double. The study exposed that “Modified pitch P2P-P” of the coil rises "overall heat transfer coefficient" by 22%.

**Xu** et.al, [10] studied the effects of various grooving approaches and depths on the heat transfer characteristics of helically coiled tube using "ANSYS FLUENT" software. The study showed that the "performance evaluation criterion" (PEC) value of the helical grooved tube was 25% higher than helical tube.

## .3. Aim of research

Study the effect of change curvature ratio and coil pitch of helical tube on heat transfer rate and oil outlet temperature.

## 4.Shell and helical tube heat exchanger model

The heat exchanger of interest in this study consists of a helical tube embedded in a cylindrical shell. Air enters the helical tube at temperatures of (200, 225 and 250) °C with velocity changes from (20 - 48) m/s while, in shell side cold fluid (oil) "flow rate" is varying from (0.06 - 0.1) kg/s with inlet temperature 40 °C. The geometry of helical heat exchanger has been made in ANSYS FLUENT 2019 R2. The geometric strictures interrelated to the shell are constant (length 1500 mm and 152.4 diameter) and two helical tube parameters including coil diameter (Dc) and pitch of helical tube (p) are variable are shown in "Figure (2)". The helical tube heat exchanger is made up of copper and air "has been used as working fluid" inside coil and heavy oil in the shell side.
as they were divided helical tube into two groups, as shown in Tables 1 and 2.

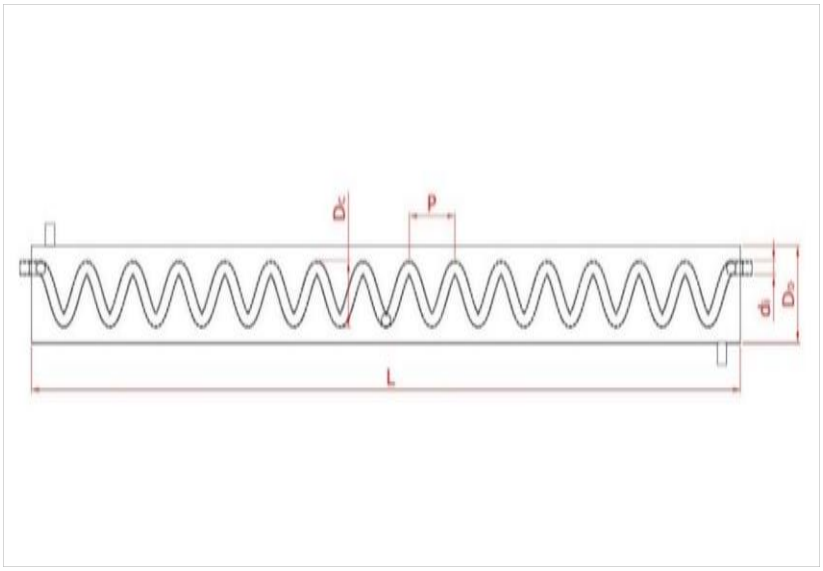


Fig.2 Shell and helical tube heat exchange geometry

Table 1 First group of helical coils (different curvature ratio)

| Specification | Coil 1 | Coil 2 | Coil 3 |
|---|---|---|---|
| diameter of coil (Dc) mm | 120 | 130 | 140 |
| diameter of tube (di) mm | 20 | 20 | 20 |
| Pitch mm | 30 | 30 | 30 |
| curvature ratio δ | 0.166 | 0.153 | 0.142 |
| No of turn | 50 | 50 | 50 |
| Length of coil m | 18.89 | 20.46 | 22 |
| $D_h$ (shell) m | 0.102 | 0.094 | 0.086 |
| A coil $m^2$ | 1.186 | 1.28 | 1.38 |

Table 2 Second group of helical coils (different pitch)

| Specification | Coil 1 | Coil 2 | Coil 3 | Coil 4 |
|---|---|---|---|---|
| diameter of coil (Dc) mm | 140 | 140 | 140 | 140 |
| diameter of tube (di) mm | 20 | 20 | 20 | 20 |
| Pitch mm | 30 | 50 | 75 | 100 |
| No of turn | 50 | 30 | 20 | 15 |
| curvature ratio δ | 0.142 | 0.142 | 0.142 | 0.142 |
| Length of coil m | 22 | 13.27 | 8.9 | 6.7 |
| $D_h$ (shell) m | 0.086 | 0.143 | 0.215 | 0.286 |
| A coil $m^2$ | 1.38 | 0.83 | 0.56 | 0.42 |

## 4.1 Mesh Generation

The process of creating the appropriate mesh is a basis CFD simulation, in order to improve the simulation's accuracy. Due to the precise mesh being produced by a proper 3D model, which also lowers the number of iterations, complex geometries are breaking down into parts that may be utilized to discretize a domain. Initially a relatively coarser mesh is generated. In the current work, a mixed of Hexa-Tetra, wedges mesh was used as shown in "Figure (3)".

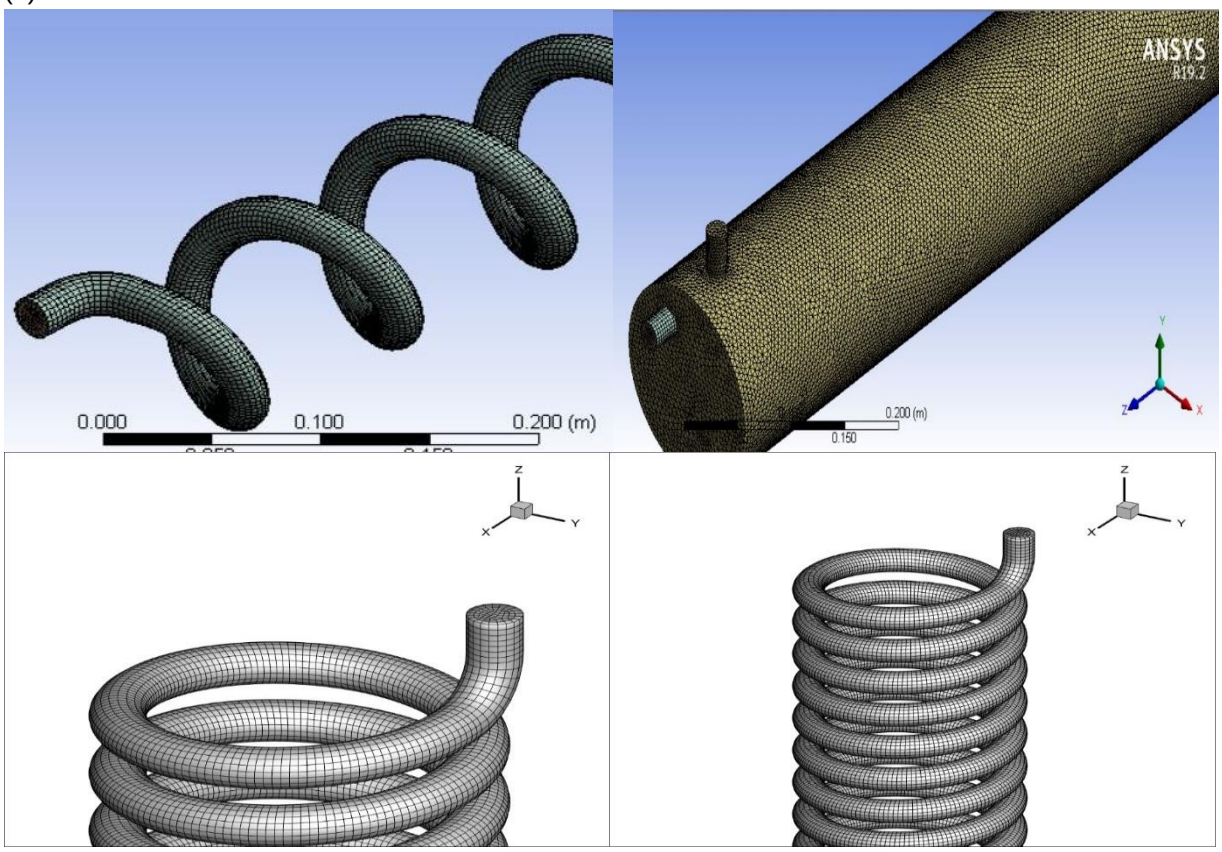


Fig. 3 Mesh of shell and helical tube heat exchange

## 4.2 Grid Independency

To confirm the accuracy of the solution, the mesh of the current study was examined by a change in some parameters and repeats the simulation work as shown in Table 3.

Table 3 Number of elements and oil outlet temperature

| Grid sizing | Element Size (mm) | No. Elements | Oil Outlet Temperature (◦c) |
|---|---|---|---|
| Coarse | 10 | 2149952 | 50.4 |
| | 8 | 2217555 | 51.3 |
| Medium | 7 | 2331760 | 52.5 |
| | 6 | 2578720 | 53.2 |
| Fine | 5 | 3161006 | 54.3 |
| | 4.5 | 3448657 | 54.5 |
| | 4 | 3769861 | 54.6 |

It is clear that the results variations are not significant after elements number 3161006 for this reason this number of elements was chosen as shown in Table 3.

## 4.3 Assumption

In order to solve the Navier-Stoke equations which are included a number of variables that can be reduced by adopting the assumptions: "Three-dimensional design", steady state, flow is turbulent in helical tube, flow is laminar in shell, incompressible flow in shell, Newtonian fluid, single phase model, adiabatic process (no heat losses) and heat exchanger is vertical and gravity is defined as y = (-9.81m/ $s^2$).

### 4.3.1 Governing Equations

The set of the differential form of equations describes the transport of mass, momentum and energy in a fluid is in the following form [10]

#### 4.3.1.1 Mass conservation (continuity equation)

$$"\frac{\partial \bar{u}}{\partial x}+\frac{\partial \bar{v}}{\partial y}+\frac{\partial \bar{w}}{\partial z}=0" \quad (1$$

#### 4.3.1.2 Conservation of Momentum

$$\left(\bar{u}\frac{\partial \bar{u}}{\partial x}+\bar{v}\frac{\partial \bar{u}}{\partial y}+\bar{w}\frac{\partial \bar{u}}{\partial z}\right)+\left(\frac{\partial}{\partial x}\left(\overline{u'^2}\right)+\frac{\partial}{\partial y}\left(\overline{u'v'}\right)+\frac{\partial}{\partial z}\left(\overline{u'w'}\right)\right)=-\frac{1}{\rho}\frac{\partial p}{\partial x}+$$

$$\frac{\mu}{\rho}\left(\frac{\partial^2 \bar{u}}{\partial x^2}+\frac{\partial^2 \bar{u}}{\partial y^2}+\frac{\partial^2 \bar{u}}{\partial z^2}\right) \quad (2)$$

$$"\left(\bar{u}\frac{\partial \bar{v}}{\partial x}+\bar{v}\frac{\partial \bar{v}}{\partial y}+\bar{w}\frac{\partial \bar{v}}{\partial z}\right)"+"\left(\frac{\partial}{\partial x}\left(\overline{u'v'}\right)+\frac{\partial}{\partial y}\left(\overline{v'^2}\right)+\frac{\partial}{\partial z}\left(\overline{u'w'}\right)\right)"=-\frac{1}{\rho}\frac{\partial p}{\partial y}+\frac{\mu}{\rho}"\left(\frac{\partial^2 \bar{v}}{\partial x^2}+\frac{\partial^2 \bar{v}}{\partial y^2}+$$

$$\frac{\partial^2 \bar{v}}{\partial z^2}\right)" \quad (3)$$

$$"\left(\bar{u}\frac{\partial \bar{w}}{\partial x}+\bar{v}\frac{\partial \bar{w}}{\partial y}+\bar{w}\frac{\partial \bar{w}}{\partial z}\right)"+"\left(\frac{\partial}{\partial x}\left(\overline{u'w'}\right)+\frac{\partial}{\partial y}\left(\overline{u'v'}\right)+\frac{\partial}{\partial z}\left(\overline{w'^2}\right)\right)"=-\frac{1}{\rho}\frac{\partial p}{\partial z}\frac{\mu}{\rho}"\left(\frac{\partial^2 \bar{w}}{\partial x^2}+\frac{\partial^2 \bar{w}}{\partial y^2}+\frac{\partial^2 \bar{w}}{\partial z^2}\right)" \quad (4)$$

### 4.3.1.3 Conservation of Energy

$$"\left(\bar{u}\frac{\partial \bar{T}}{\partial x}+\bar{v}\frac{\partial \bar{T}}{\partial y}+\bar{w}\frac{\partial \bar{T}}{\partial z}\right)"+"\left(\frac{\partial}{\partial x}(\overline{u'T'})+\frac{\partial}{\partial y}(\overline{v'T'})+\frac{\partial}{\partial z}(\overline{w'T'})\right)"=\alpha"\left(\frac{\partial^2 \bar{T}}{\partial x^2}+\frac{\partial^2 \bar{T}}{\partial y^2}+\frac{\partial^2 \bar{T}}{\partial z^2}\right)" \quad (5)$$

## 4.3.2 Model

Using the energy equation and the viscous k-epsilon models from Fluent, Realizable because it can employ two equations of k- to increase the precision of the eddy's flows and the quickly exhausted flows.

### 4.3.2.1 Turbulence Kinetic Energy Equation

$$\rho"\left(\bar{u}\frac{\partial k}{\partial x}+\bar{v}\frac{\partial k}{\partial y}+\bar{w}\frac{\partial k}{\partial z}\right)"="\left[\left(\mu+\frac{\mu_t}{\sigma_k}\right)\left(\frac{\partial^2 k}{\partial x^2}+\frac{\partial^2 k}{\partial y^2}+\frac{\partial^2 k}{\partial z^2}\right)\right]"+G_k-\rho\epsilon \quad (6)$$

### 4.3.2.1 Dissipation Rate ( ∈ ) Equation

$$\rho"\left(\bar{u}\frac{\partial \epsilon}{\partial x}+\bar{v}\frac{\partial \epsilon}{\partial y}+\bar{w}\frac{\partial \epsilon}{\partial z}\right)"="\left[\left(\mu+\frac{\mu_t}{\sigma_\epsilon}\right)\left(\frac{\partial^2 \epsilon}{\partial x^2}+\frac{\partial^2 \epsilon}{\partial y^2}+\frac{\partial^2 \epsilon}{\partial z^2}\right)\right]"+C_{1\epsilon}\frac{\epsilon}{k}G_k-C_{2\epsilon}\rho\frac{\epsilon^2}{k} \quad (7)$$

## 3.3.3 Materials

In the current work, the properties of the materials must be entered if they are fluid or solid to be recognized by the program as shown in Table 4.

Table 4 Properties of materials

| Materials | "Density" kg/$m^3$ | "(specific heat)" J/kg. k | "Thermal conductivity" (w/m. k) | "Viscosity" (kg/m. s) |
|---|---|---|---|---|
| **Air** | 1.225 | 1006.34 | 0.0242 | $1.7894\times10^{-5}$ |
| **Heavy oil** | 960 | 1880 | 0.12 | 0.048 |
| **Copper** | 8978 | 381 | 387.6 | |

## 4.3.4 Boundary Condition

The boundary conditions which are applied in this study are listed in the following Table 5.

Table 5 Boundary condition for air and heavy oil.

| | | |
|---|---|---|
| **Inlet boundary condition for air** | | |
| **1** | Temperature | (200,225,250) ºC |
| **2** | Inlet velocities | (20,27,34,41,48) m/s |
| **Inlet boundary condition for heavy oil** | | |
| **1** | Temperature | 40 ºC |
| **2** | mass flow rate | (0.06, 0.08, 0.1) kg/s |
| **Pipe wall boundary condition** | | |
| **Inner pipe** | Thermal condition | Via system coupling |
| | Material | Copper |
| **Outer pipe** | Thermal condition | Via system coupling |
| | Material | Copper |
| **Adiabatic wall** | Heat Flux | 0 W/$m^2$ |

## 5.DATA REDUCTION

Heat transfer from the hot fluid is equal to the cold fluid

$$Q = \dot{m}_h \times C_{ph} \times \Delta t \quad (8)$$

$$Q = \dot{m}_c \times C_{pc} \times \Delta t \quad (9)$$

Helical Tube Side (air):

$$Q = U_i A_i \Delta T_{lmt} = U_o A_o \Delta T_{lmtd} \quad (10)$$

$$A_i = \pi d_i L_c \quad (11)$$

$$L_c = N\sqrt{(\pi D_c)^2 + (p)^2} \quad (12)$$

$$LMTD = \frac{\Delta T1 - \Delta T2}{Ln\left(\frac{\Delta T1}{\Delta T2}\right)} \quad (13)$$

$$\Delta T1 = Th_1 - Tc_2 \quad (14)$$

$$\Delta T2 = Th_2 - Tc_1 \quad (15)$$

Turbulent Nusselt number [11]

$$Nu = 0.023\ Re^{0.85} Pr^{0.4} \left(\frac{d_i}{D_c}\right)^{0.1} \quad (16)$$

$$Re = \frac{\rho\, u\, d_i}{\mu} \quad (17)$$

$$Pr = \frac{\mu_{air} cp_{air}}{k_{air}} \quad (18)$$

$$h_i = \frac{Nu\, k}{d_i} \quad (19)$$

$$De = Re \left(\frac{d_i}{D_c}\right)^{0.5} \quad (20)$$

$$\because Q = \dot{m}_c \times C_p \times \Delta t \quad (21)$$

$$U_o = \frac{Q}{A_o \Delta T_{lmtd}} \quad (22)$$

$$U_o = \frac{1}{\frac{A_o}{h_i A_i} + \frac{A_o \ln\left(d_o/d_i\right)}{2\pi K_t L} + \frac{1}{h_o}} \quad (23)$$

$$d_h = \frac{D_{sh}^2 - \pi D_c d_i^2 \gamma^{-1}}{D_{sh} + \pi D_c d_i\ \gamma^{-1}} \quad [12] \quad \text{shell side} \quad (24)$$

$$\gamma = \frac{p}{\pi D_c} \quad (25)$$

$$Nu = \frac{h_o d_h}{K} \quad (26)$$

$$\varepsilon = \frac{Q_{actual}}{Q_{max}} \quad (27)$$

# 6.RESULTS AND DISCUSSION

Numerical investigations" have been carried out to study the effect of "oil mass flow rate", pitch, and coil diameter on heat transfer and flow features in a "shell and helical tube heat exchanger". The flow is turbulent in helical tube and laminar in shell and flow arrangement is counter flow. The number of iterations is set to 1000 and when the solution is converged, temperature, pressure for air and oil are calculated from reports – surface integral – facet average.

## 6.1 Validation of numerical results

To ensure the theoretical findings are accurate, a comparison was made with the experimental results of the previous study. The study presented by the researcher was selected from Kumar et al. (2020) attended as references to the experimental literature data that were made for validation. The working fluid water was allowable to flow at three dissimilar flow rates of "(1, 2, and 3) l/min" at temperature of 298 k on shell side and at "(1, 1.5, 2, 2.5, and 3) l/min" and temperature of (323±0.4 K) on coil side (hot water). Temperature difference was calculated and plotted against the volume flow rate as shown on the other hand, Nusselt Number was calculated which it is plotted against the inner Dean number and compared with present study. "Figure (4)" evident that the present prediction is in agreement with the results by Kumar et al. (2020) with a small average deviation 1.1% and 2% between the values. However, the results behavior was similar.

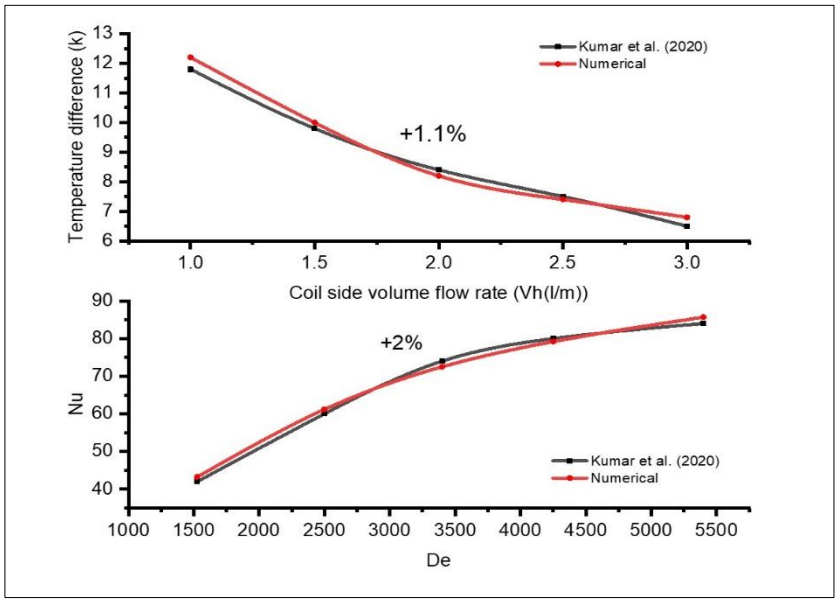


Fig. 4 Validation numerical results with experimental result of previous study

## 6.2 Effect of oil flow rate on heat transfer rate and oil temperature

From "Figure (5)" the results indicate that "oil outlet temperature" decreased about 3% with increase of "oil flow rate" from (0.06 - 0.1) kg/s. The reason is the mass flow rate is a function of the fluid velocity, so low mass flow rate means low velocity and that mean more time for the fluid particles to pass throw the heat exchanger form inlet point to the exit point. This additional time give these particles to get higher temperature. Also, increasing "oil mass flow rate" cause increasing in heat transfer with percentage 37% because the increasing of flow rate led to increases oil heat capacity. Also, Nusselt number and convective heat transfer coefficient for air side not affected and it's almost the same.

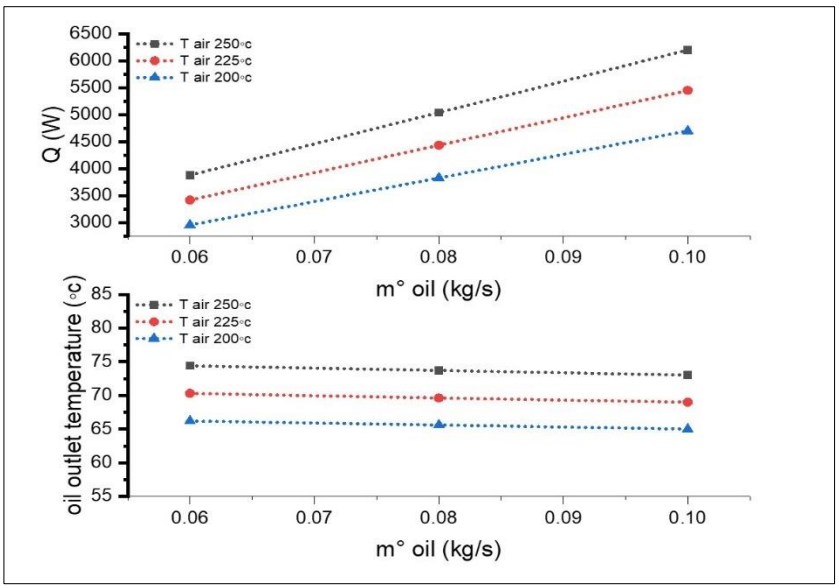


Fig.5 Effect of oil flow rate on heat transfer rate and oil outlet temperature

## 6.3 Effect of curvature ratio

Curvature ratio is the ratio of the inner helical tube diameter (di) to the diameter of the coil. It creates stronger centrifugal force that leads to increase maximum axial velocity and secondary velocity [15]. In this part the effect of changing curvature ratio will be discussed based on the specifications in Table 1, the diameter of coil Dc has been changed (120,130 and140) mm, coil pitch 30 mm at constant oil flow rate 0.06 kg/s and constant air inlet temperature 250 $^{o}$C**.**

### 6.3.1 Effect of curvature ratio on Dean number

Dean number (De) is a function of "Reynolds number" (Re) and curvature ratio. As shown in "Figure (6)". The results show that Dean number (De) for air side increased with percentage 58 % when (Re) increased from minimum value 26014 to maximum value 62434 at constant curvature ratio **(δ).** Also, Dean number is higher in coil (1) with curvature ratio 0.166 than coil (2) and coil (3) with percentage (4%, 8%) respectively due to increase curvature ratio leads to increase centrifugal force and secondary flow.

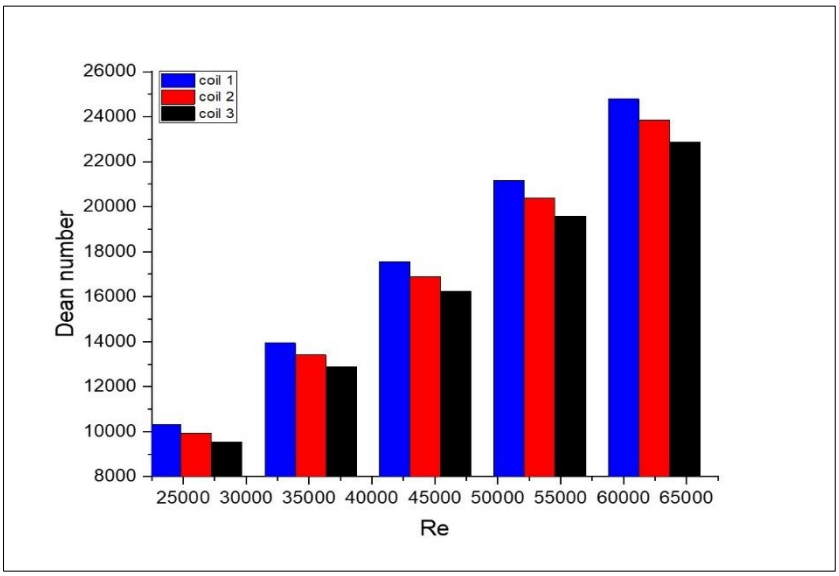


Fig.6 Effect of curvature ratio on Dean number

### 6.3.2 Effect of curvature ratio on heat transfer rate and oil outlet temperature

"Figure (7)" shows variation in heat transfer and temperatures of oil for different curvature ratio. It is clear that maximum oil outlet temperature and maximum heat transfer rate at coil (3) with curvature ratio 0.142 because the surface area of this coil is slightly higher than coil (1) and coil (2). So, heat transfer rate and oil outlet temperature are higher in coil (3) with percentage (12%, 6%) and (5%, 3%) than coil (1) and coil (2) respectively.

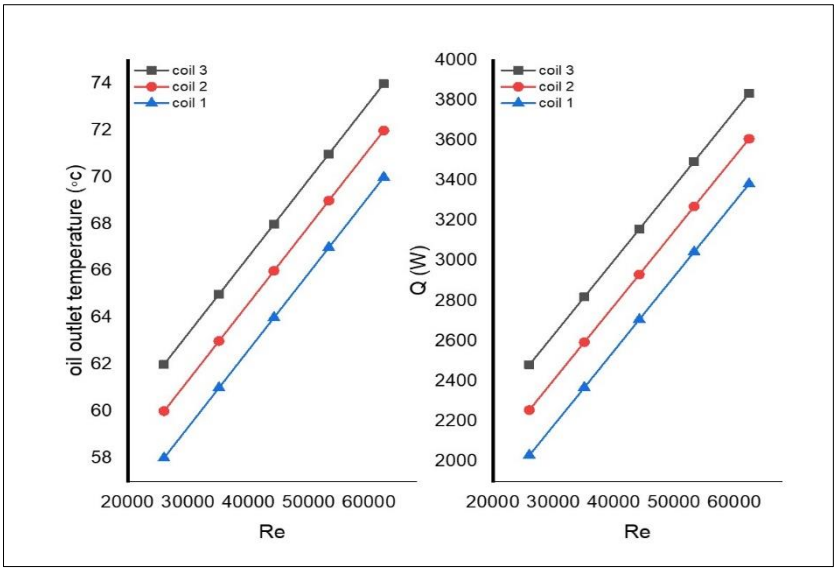


Fig .7 Effect of curvature ratio on heat transfer and oil outlet temperature

### 6.3.3 Effect of curvature ratio on Nusselt number

It is known that De is directly proportional to Nusselt number (Nu). As a result, Nu decreases with the increase of coil diameter. Additionally, this can be accredited to the increase of Nu in helical tube which is related to the detail that in higher De, stronger "secondary flows" will be gotten that are innovative in the cross section of tube. Therefore, the momentum transmission from wall of the tube increases and as a result of having developed momentum argument near the wall [16]. "Figure (8)" shows that Nu in helical coil (air side) higher in coil (1) than coil (2) and coil (3) due to increasing Re but the effect of changing curvature ration is not significant while in shell (oil side) it is higher in coil (1) with percentage (11%, 21%) than coil (2) and coil (3) respectively.

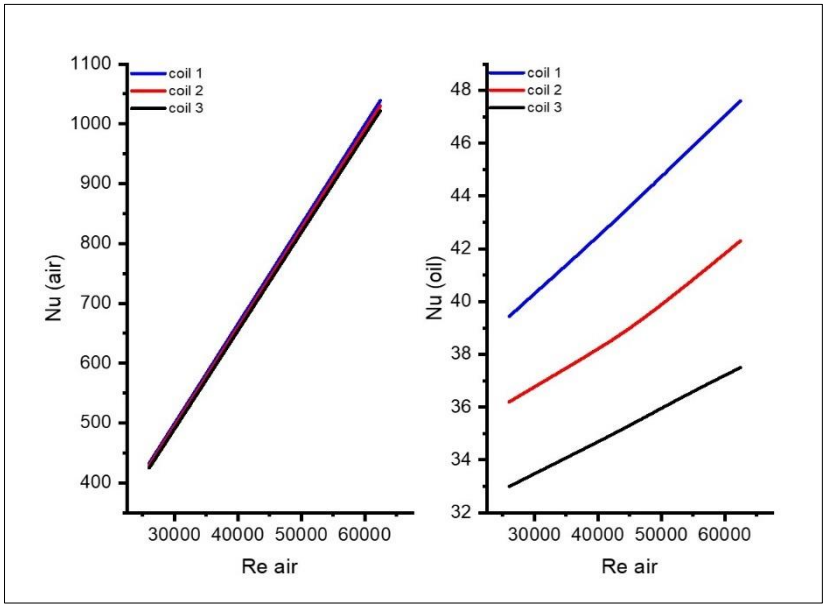


Fig.8 Effect of curvature ratio on Nusselt number

### 6.3.4 Effect of curvature ratio on overall heat transfer coefficient and effectiveness

From "Figure (9)" it is clear that "overall heat transfer coefficient" and "effectiveness of shell and helical tube" heat exchanger enhance with increased Re and coil diameter because at high Re the whirlpool creation has capability to destroy thermal boundary layer, Also "heat transfer rate" increased as a result of increase surface area of the thermal exchange therefore higher "overall heat transfer coefficient" and "effectiveness" at coil (3) with percentage (27%,15%) and (12%,6%) respectively compared with coil (1) and coil (2)

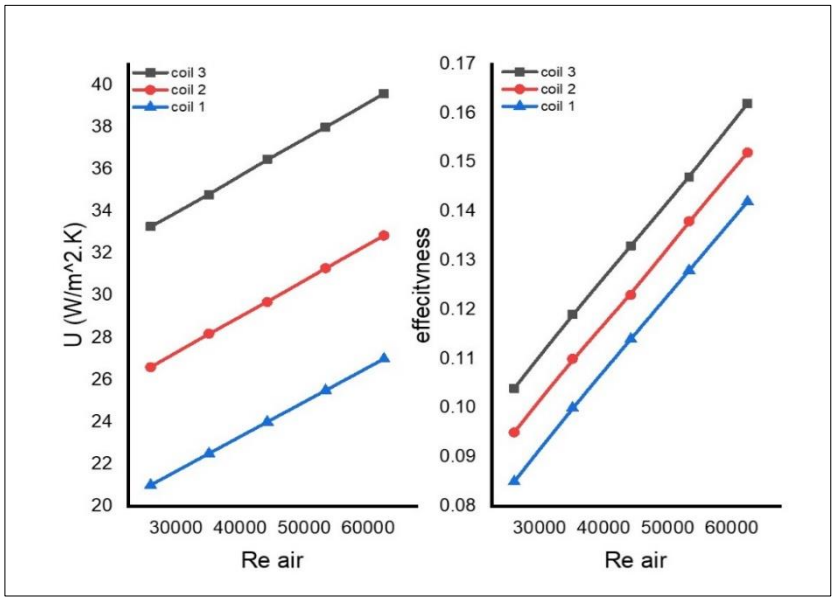


Fig.9 Effect of curvature ratio on overall heat transfer coefficient and effectiveness

## 6.4 Effect of coil pitch

In this part, the effect of change coil pitch (30,50,75 and 100) mm on the thermal performance of the heat exchanger will be studied based on the specifications in Table 2 at constant oil flow rate 0.06 kg/s and constant air inlet temperature 250 $^{o}$C and know the effect of each pitch on heat transfer rate and oil outlet temperature and other parameter.

### 6.4.1 Effect of coil pitch on heat transfer rate

As can be seen in "Figure (10)", the flow within the coil with the largest number of turn (pitch 30 mm) revelations a greater "heat transfer rate". Pitch also affects the "centrifugal force" on a fluid in motion. From figure it is clear that maximum heat transfer rate at coil pitch 30 mm and it is a higher with percentage (6%,10%,17%) respectively than other coils because the surface area of this coil is largest**.** Also, heat transfer rate increase about 35% when Dean number increases from 9547 to 22879.

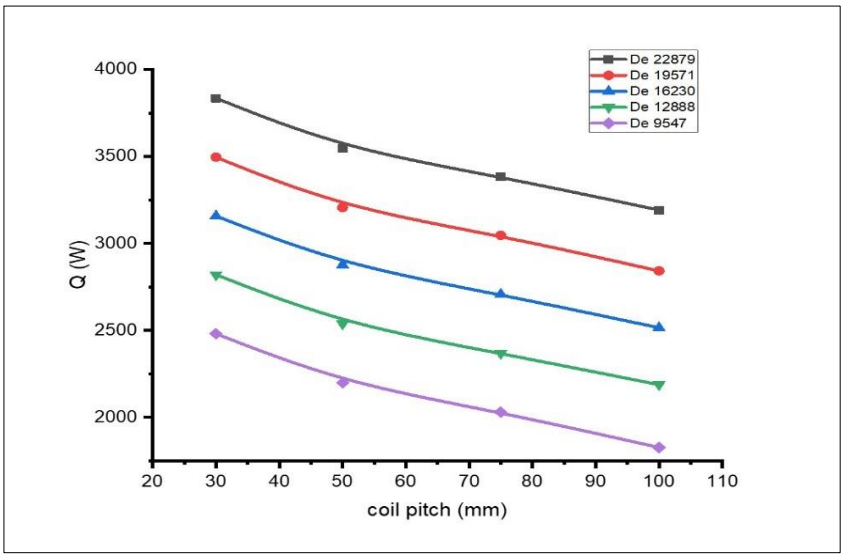


Fig.10 Effect of coil pitch on heat transfer rate

## 6.4.2 Effect of coil pitch on oil outlet temperature

The effect of coil pitch on oil temperature difference between inlet and outlet coil side shown in "Figure (11)" it can be seen that the maximum difference of temperature appears at the coil with pitch 30 mm. "Coil pitch" and Dean number have significant effect on the value of oil temperature. These values decrease with increasing coil pitch and increases with increasing Dean number at the same inlet condition. Generally maximum oil outlet temperature at coil (1) with pitch 30 mm and Dean number 22879 and minimum oil outlet temperature at coil (4) with pitch 100 mm and Dean number 9547.

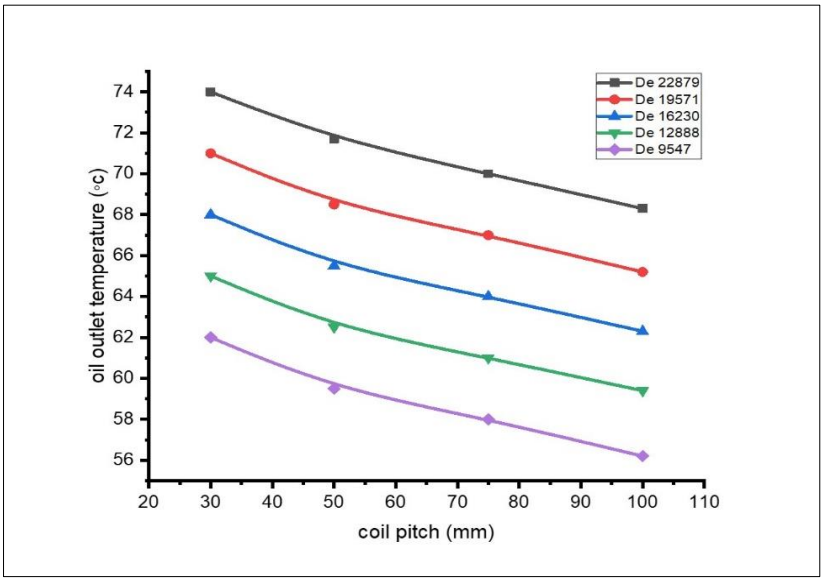


Fig.11 Effect of coil pitch on oil outlet temperature

### 6.4.3 Effect of coil pitch on Nusselt number

"Figure (12)" shows relationship between De (air side) and Nu" (oil side). From the results the heat transfer coefficient" and Nu inside shell enhance with increase coil pitch because in smaller coil pitches, the oil is kept in the space between the sequential coil circles and semi-dead zone is formed and in this region, the flow slowed and heat transfer coefficients will be down .for this reason maximum Nu in coil (4) with pitch 100 mm and it is a higher about ( 32%,69%,74%) compared with coil (3) ,coil (2) and coil (1) respectively .Also, "Nusselt number" in shell side increase about 7% when "Dean number" increases from 9547 to 22879 and increasing pitch coil does not cause significant change on Nusselt number of air side.

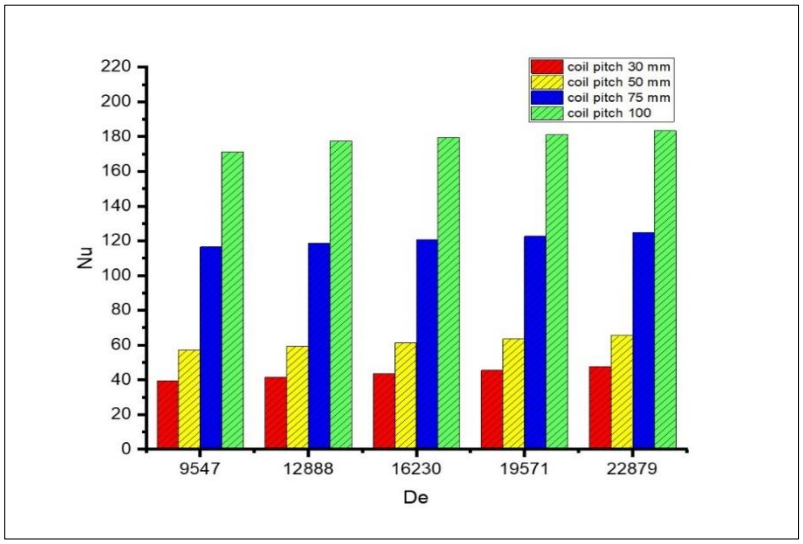


Fig.12 Effect of coil pitch on Nusselt number

### 6.4.4 Effect of coil pitch on overall heat transfer coefficient

"Figure (13)" shows variation of "overall heat transfer coefficient" at different coil pitch. It appeared that the increase of coil pitch led to increase "overall heat transfer coefficient" and this increment was high for the pitch change from 50 mm to 100 mm but on increasing the pitch beyond 50 mm the increment was moderate. As a result of increasing coil pitch the log mean temperature difference (LMTD) decrease and surface area of coil decrease too for this reason "overall heat transfer coefficient" increased and maximum "overall heat transfer coefficient" in coil (4) with pitch 100 mm and it is a higher about (16%,36%,42%) compared with coil (3), coil (2) and coil (1) respectively

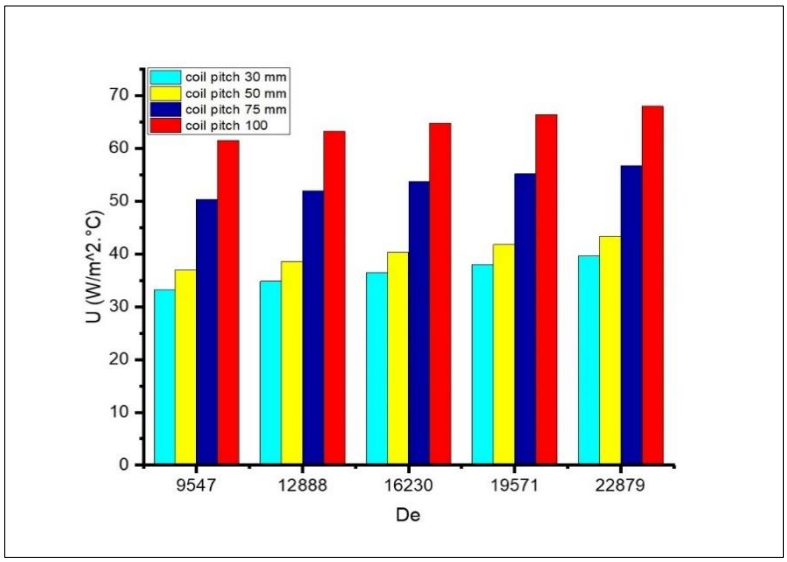


Fig.14 Effect of coil pitch on overall heat transfer coefficient

## 6.4.5 Effect of coil pitch on effectiveness

"Figure (14)" shows influence Dean number on effectiveness of heat exchanger at different coil pitch. It seemed maximum effectiveness in coil (1) with pitch 30 mm and it is a higher about (7%,12%,17%) compared with coil (2), coil (3) and coil (4) respectively. It is clear the effectiveness decreased with increased coil pitch due to decrease actual heat transfer rate. Also, effectiveness increased about 35% when dean number increased from 9547 to 22879.

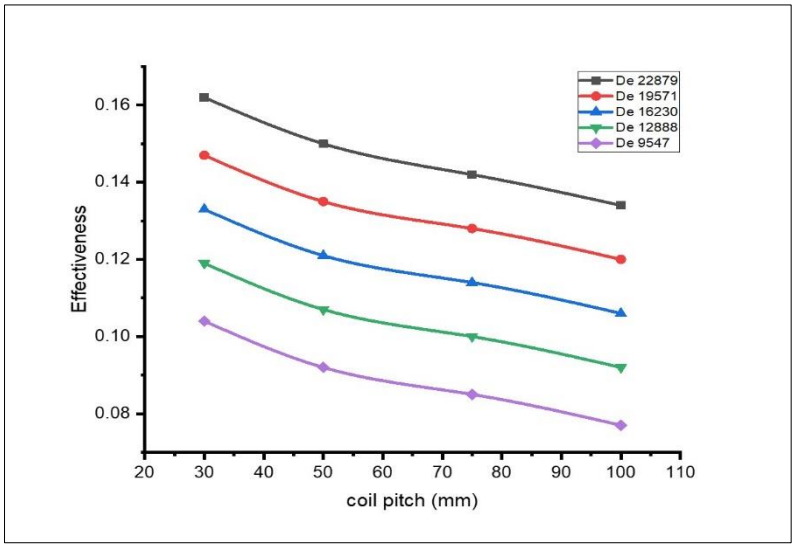


Fig.14 Effect of coil pitch on effectiveness

## 6.4.6 Effect of coil pitch on pressure drops

Friction is a main cause of pressure drops. Friction occurs inside wall of pipe when fluid passages in these pipes. Pressure drop is a function of friction factor and length of pipe and increase pitch led to decrease length. Therefore, maximum oil pressure drops in coil (1) with pitch 30 mm and it is a higher than coil (2), coil (3) and coil (4) with (3%,6%,8%) respectively as shown in "figure (15)" while the values of air pressure drops remain nearly unchanged with increased coil pitch

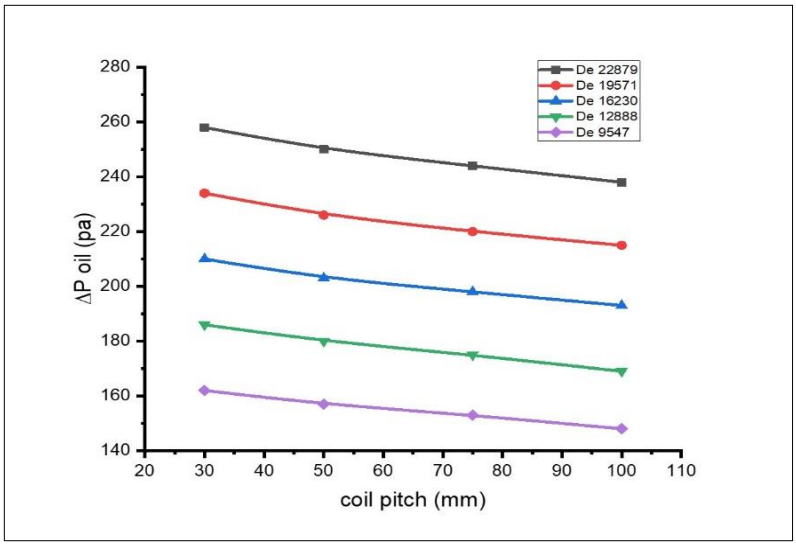


Fig.15 Effect of coil pitch on pressure drops

## 6.5 Temperature Contour

The effects of different curvature ratio on the temperature distribution are shown in "figure (16.a)". It can be seen that the maximum difference of temperature appears at the coil (3) with curvature ratio 0.142. Oil outlet temperature in coil (3) is slightly higher than that with coil (1) and coil (2). Furthermore, the temperatures of oil increase with increasing coil diameter Dc, which indicates that a larger amount of heat is transferred to the shell from the helical tube and maximum temperature occurs at the centre of tube.

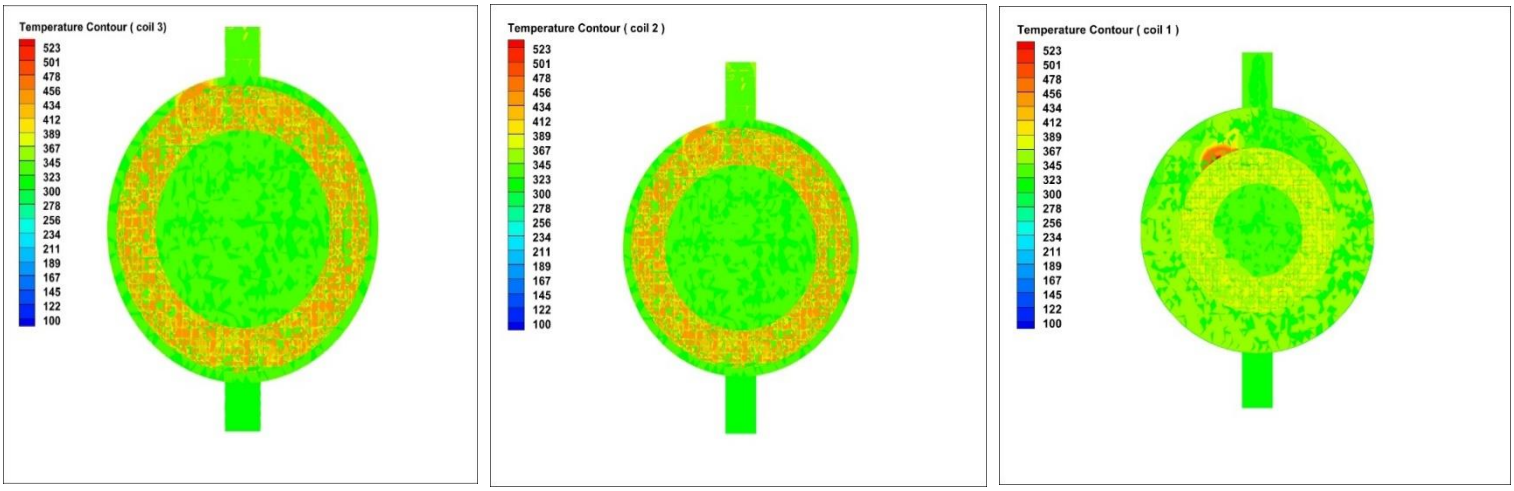


c. curvature ratio 0.142 b. curvature ratio 0.153 a. curvature ratio 0.166

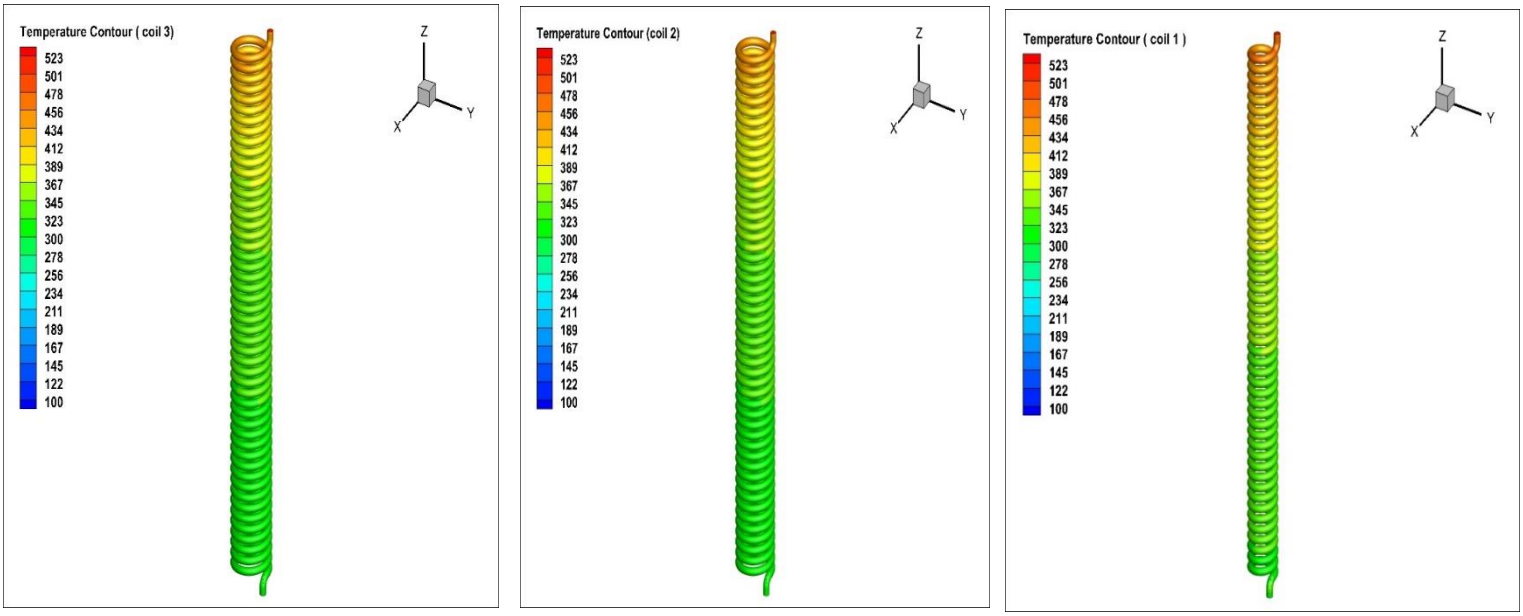


g. curvature ratio 0.142 f. curvature ratio 0.153 e. curvature ratio 0.166

Fig. 16.a Temperature Contour at different curvature ratio

From "Figure (16. b)" at (xyz) plain it can be seen that hot temperature difference decrease with increase coil pitch and maximum heat transfer rate in helical coil with pitch 30 mm.

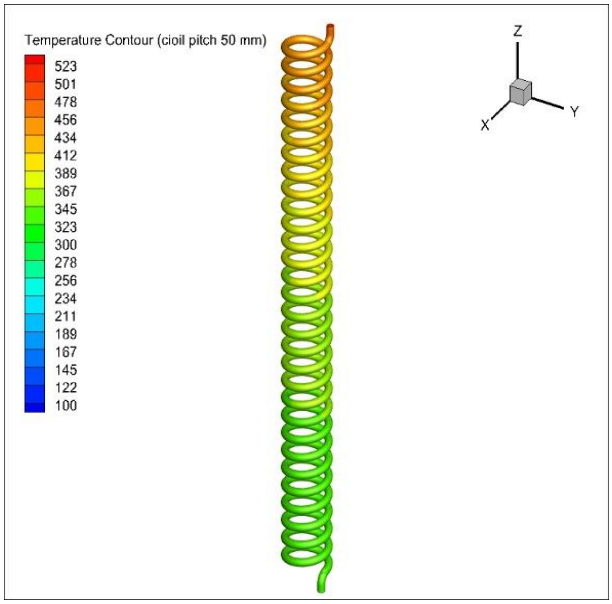


b. coil pitch 50 mm

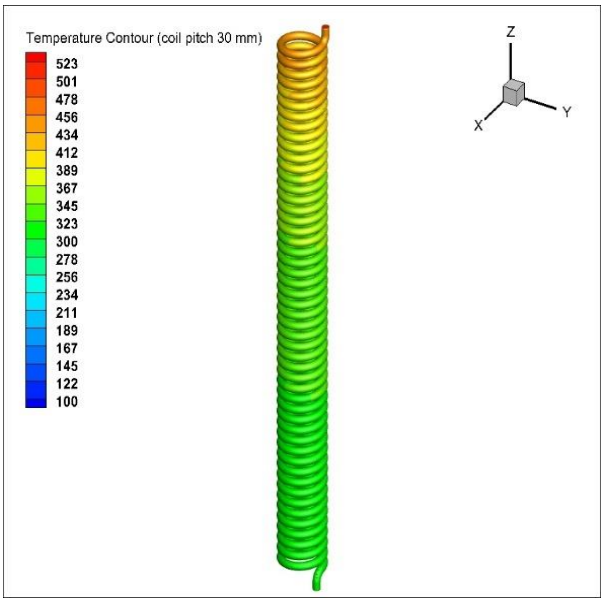


a. coil pitch 30 mm

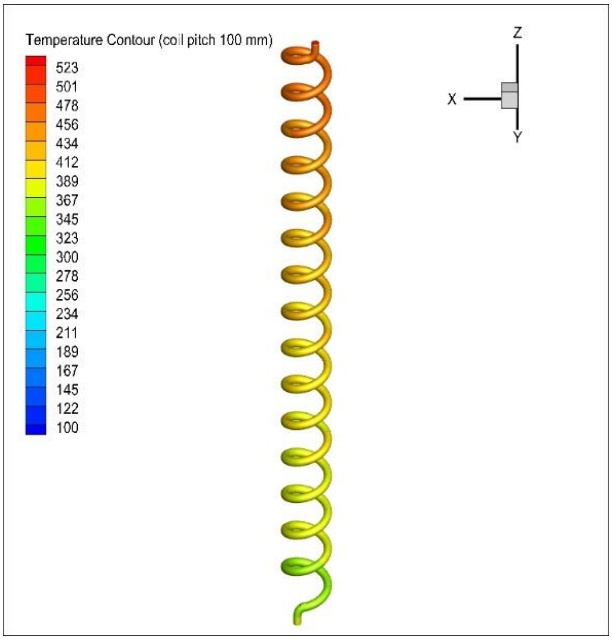


d. coil pitch 100 mm

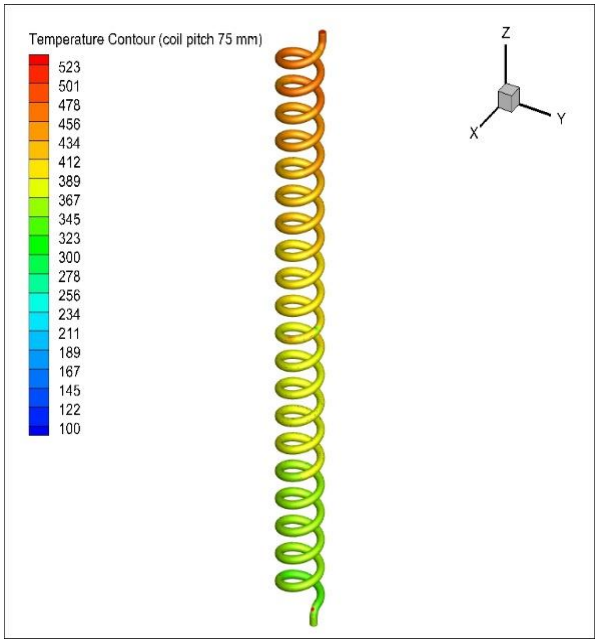


c. coil pitch 75 mm

Fig. 17.b Temperature Contour at different coil pitch

## 6.6 Performance of heat exchanger

In order to investigate the effect of using helical coil a detailed comparison is first made between the straight tube and helical coil. Here, it is expected that they have a higher heat transfer rate and pressure loss compared to the smooth tubes. It is known that higher Nusselt numbers and lower friction factor coefficients are needed to have cases with higher performance, Performance Evaluation Criterion (PEC) is used in this part to simultaneously consider the effects of higher heat transfer rate and pressure loss which is defined as the following:

$$PEC = \frac{(\frac{Nu}{\mathrm{Nus}})}{(\frac{f}{fs})^{0.33}}$$

where Nu and f respectively stand for Nusselt number and friction factor coefficient of the straight tube. From "Figure (18)" It is observed that Performance Evaluation Criterion increased with increase coil pitch and Dean number. The highest performance at coil pitch (75 and 100) mm and case with coil pitch = 100 mm offers the maximum performance among the investigated cases.

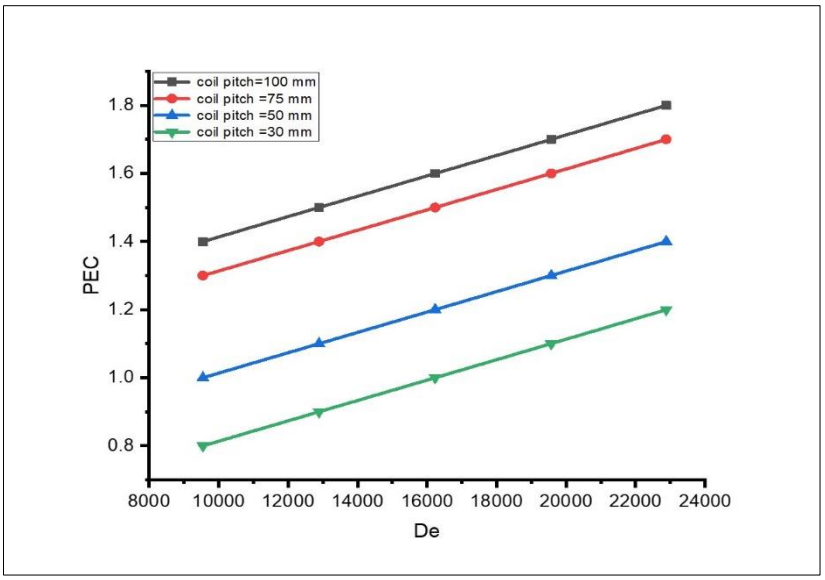


Fig.18 Performance Evaluation Criterion (PEC) at different coil pitch

## 7.CONCLUSIONS

In this study, numerical simulations were showed to study "heat transfer enhancement" of "shell and helical tube heat exchanger", and influence of increase oil flow rate, curvature ratio and coil pitch on heat transfer concert of the heat exchanger and oil outlet temperature. The next conclusions can be drawn from the annotations:

1- Increasing "oil mass flow rate" from (0.06 to 0.1) kg/s cause decreasing oil outlet temperature about 3% and increasing heat transfer rate with 37%.
2- Increasing curvature ratio leads to increase centrifugal force, secondary flow and. Dean number.
3- Heat transfer rate and oil outlet temperature are higher in coil (3) with curvature ratio 0.142 about (12%, 6%) and (5%, 3%) than curvature ratio 0.153 and 0.166 respectively.
4- Nusselt number (oil side) is higher in coil (1) with curvature ratio 0.166 about (11%, 21%) compared with curvature ratio 0.153 and 0.142 respectively.
5- Heat transfer rate increase 35% and oil outlet temperature increases 22% when Dean number increases from 9547 to 22879.
6- Heat transfer rate and oil outlet temperature decrease with increase coil pitch about (17% and 8%) respectively.
7- Overall heat transfer coefficient increased with decreasing curvature ratio and increased with decreased coil pitch.
8- Effectiveness of heat exchanger increased with decreasing curvature ratio and decreasing with increase coil pitch.
9- Nusselt number enhance with increase pitch coil and it is a higher in pitch 100 mm about (32%,69%,74%) compared with pitch (75,50 and 30) mm and increasing coil pitch does not cause significant change on Nusselt number of air side.
10- Maximum oil pressure drops in coil (1) with pitch 30 mm and it decreases with increase coil pitch.
11- The highest Performance Evaluation Criterion (PEC) at coil pitch (75 and 100) mm and case with coil pitch = 100 mm offers the maximum performance among the investigated cases.

## References

[1] S. C. R. DENNIS, MICHAEL NG, DUAL SOLUTIONS FOR STEADY LAMINAR FLOW THROUGH A CURVED TUBE, *The Quarterly Journal of Mechanics and Applied Mathematics*, Volume 35, Issue 3, August 1982, Pages 305–324.

[2] “Helical Coil Heat Exchanger Design.” https://www.lizhengcoils.com/single-post/2015/08/20/helical-coil-heat-exchanger-design (accessed Feb. 02, 2023).

[3] A. Sheeba, C. M. Abhijith, and M. Jose Prakash, “Experimental and numerical investigations on the heat transfer and flow characteristics of a helical coil heat exchanger,” *Int. J. Refrig.*, Vol. 99, pp. 490–497, 2019, doi: 10.1016/j.ijrefrig.2018.12.002.

[4] R. A. Rezaei, S. Jafarmadar, and S. Khorasani, “Presentation of frictional behavior of micro helical tubes with various geometries and related empirical correlation; an experimental study,” *Int. J. Therm. Sci.*, Vol. 140, No. November 2018, pp. 377–387, 2019, doi: 10.1016/j.ijthermalsci.2019.03.011.

[5] N. Kushwaha, Vikash, and V. Kumar, “Impact of Mixed Convective and Radiative Heat Transfer in Spiral-Coiled Tubes,” *J. Heat Transfer*, Vol. 141, No. 8, pp. 1–10, 2019, doi: 10.1115/1.4043946.

[6] R. Kumar, P. Chandra, and Prabhansu, “Innovative method for heat transfer enhancement through shell and coil side fluid flow in shell and helical coil heat exchanger,” *Arch. Thermodyn.*, Vol. 41, No. 2, pp. 239–256, 2020, doi: 10.24425/ather.2020.133631.

[7] N. H. Abu-Hamdeh *et al.*, “A detailed hydrothermal investigation of a helical micro double-tube heat

exchanger for a wide range of helix pitch length," *Case Stud. Therm. Eng.*, Vol. 28, No. August, p. 101413, 2021, doi: 10.1016/j.csite.2021.101413.

[8] A. Najm, I. Dawood Jumaah, and A. M. A. Karim, "Effect of Using A Double Coil Tube with Modified Pitch on The Overall Heat Transfer Rate," *Diyala J. Eng. Sci.*, Vol. 8716, No. 1, pp. 40–53, 2022, doi: 10.24237/djes.2022.15104.

[9] P. Xu, T. Zhou, J. Xing, J. Chen, and Z. Fu, "Numerical investigation of heat-transfer enhancement in helically coiled spiral grooved tube heat exchanger," *Prog. Nucl. Energy*, Vol. 145, No. June, p. 111896, 2022, doi: 10.1016/j.pnucene.2022.104132.

[10] Fluent Thoery Guide, "Ansys Fluent Theory Guide," *ANSYS Inc., USA*, Vol. 15317, No. November, pp. 724–746, 2013, [Online]. Available: http://scholar.google.com/scholar?hl=en&btnG=Search&q=intitle:ANSYS+FLUENT+Theory+Guide#0

[11] A. S. Puttewar and A. M. Andhare, "Design and Thermal Evaluation of Shell and Helical," pp. 416–423, 2015.

[12] Nada S., Eid E., Abd El Aziz G., Hassan H., "Heat Transfer enhancement in shell and helical coil with external radial fins," *Twelfth Int. Conf. Eng. (AEIC), AlAzhar Univ. Egypt*, Vol. 7, No. 2, pp. 350–369, 2012.

[13] H. Khosravi-Bizhaem and A. Abbassi, "Effects of curvature ratio on forced convection and entropy generation of nanofluid in helical coil using two-phase approach," *Adv. Powder Technol.*, Vol. 29, No. 4, pp. 890–903, 2018, doi: https://doi.org/10.1016/j.apt.2018.01.005.

[14] M. Omidi, M. Farhadi, and A. Ali Rabienataj Darzi, "Numerical study of heat transfer on using lobed cross sections in helical coil heat exchangers: Effect of physical and geometrical parameters," *Energy Convers. Manag.*, Vol. 176, No. July, pp. 236–245, 2018, doi: 10.1016/j.enconman.2018.09.034.

[15] M. Abdullah and A. Hussein, "Impact of coil pitch on heat transfer enhancement of a turbulent flow of α-Al2O3/DW nanofluid through helical coils," *Therm. Sci.*, No. 00, pp. 131–131, 2023, doi: 10.2298/tsci230227131a.

[16] Q. S. Mahdi, S. A. Fattah, and F. juma Abd, "Experimental and Numerical Investigation to Evaluate the Performance of Helical Coiled Tube Heat Exchanger," *J. Eng. Dev.*, Vol. 18, No. 1813–7822, pp. 89–110, 2014.